

Two-population model for MTL neurons: The vast majority are almost silent

Andrew Magyar and John Collins

Physics Department, Pennsylvania State University, University Park, PA 16802, USA

(Dated: 07 November 2014)

Recordings in the human medial temporal lobe have found many neurons that respond to pictures (and related stimuli) of just one particular person out of those presented. It has been proposed that these are concept cells, responding to just a single concept. However, a direct experimental test of the concept cell idea appears impossible, because it would need the measurement of the response of each cell to enormous numbers of other stimuli. Here we propose a new statistical method for analysis of the data, that gives a more powerful way to analyze how close data are to the concept-cell idea. It exploits the large number of sampled neurons, to give sensitivity to situations where the average response sparsity is to much less than one response for the number of presented stimuli. We show that a conventional model where a single sparsity is postulated for all neurons gives an extremely poor fit to the data. In contrast a model with two dramatically different populations give an excellent fit to data from the hippocampus and entorhinal cortex. In the hippocampus, one population has 7% of the cells with a 2.6% sparsity. But a much larger fraction 93% respond to only 0.1% of the stimuli. This results in an extreme bias in the reported responsive of neurons compared with a typical neuron. Finally, we show how to allow for the fact that some of reported identified units correspond to multiple neurons, and find that our conclusions at the neural level are quantitatively changed but strengthened, with an even stronger difference between the two populations.

I. INTRODUCTION

A long-standing debate (e.g., [4–6, 26, 27, 30, 31]) concerns whether biological neural systems use local or distributed coding¹ for the representation of high-level entities, like individual people. Although the consensus [10] is that only distributed coding is used, a number of experiments find results that are very suggestive of local coding. For example, Hahnloser, Kozhevnikov and Fee [11] find neurons in zebra finches that each fire only at one particular time during a bird’s singing of its own song. In a sensory context in the medial temporal lobe (MTL) of human epileptic patients, Quiñones Quiroga et al. [32] report many examples of neurons that fire only in response to a stimulus that contains a particular person. It has been suggested that these neurons are concept cells [29], responding to one concept out of many possible.

It is therefore important to measure how close such neurons are to the local coding situation. There are some interesting conceptual issues associated with what precisely should be meant by the previous sentence, and we will discuss these further in Sec. VII C. Among these is the question of whether a particular neuron should be considered as actually participating in the representation of a particular concept, when it is measured that the neuron responds strongly to the presence (in some sense) of

that concept in the stimulus. It might be, for example, that, instead, the neuron represents an episodic memory whose content includes the concept.

For our immediate purposes, we do not actually have to solve this issue. The problem we address is that any neuron that does local coding for a high-level concept will respond to only a very small fraction of stimuli, so that direct experimental measurements have great difficulty testing whether the coding is actually local. Consider the classic case where the concepts represented are actually those detected in a current stimulus. For example, the concept might be that of a particular individual human in a visual scene. To measure whether a particular cell implements local coding for a concept, one would need presentation of stimuli that cover a large fraction of the concepts known to the subject. This is evidently far beyond current experimental capabilities, at least. Measurements such as those in [22, 32] use stimuli corresponding to only about 100 distinct entities (people, famous buildings, etc).

As one of us has shown [9] in collaboration with Jin, a substantial complication in the interpretation of the data is that there are wide differences in the response properties of the neurons in question. A small percentage respond to several distinct stimuli out of those presented, while a vast majority respond on average to much less than one. This was quantitatively deduced from summary statistics for the data that were given in [32]. (No further breakdown of the data was given.) We made a prediction for the fraction of neurons as a function of the number of stimuli to which they make an above-threshold response.

In this paper, we present and use a more complete version of the novel statistical method underlying our earlier work, to deduce the conceptual-coding properties of neu-

¹ For our purposes, we will mean by a local code that there exist single neurons for particular concepts, ideas, or other entities, so that activity of one of these neurons above some threshold indicates exclusively the presence of the corresponding entity. With distributed coding, measurements from several or many neurons are needed to determine whether a particular entity is present.

rons. Applying it to more recent and more detailed data from [22], we will find that in fact the vast majority of the measured neurons respond on average to much less than one stimulus in the approximately 100 that are presented. A direct measurement on a single neuron would need thousands of conceptually distinct stimuli to achieve the same result. The effectiveness of our method arises from the large number of neurons probed. A measure of the method’s power is the number of neuron-stimulus trials, i.e., the number of stimuli times the number of neurons. This is in the hundreds of thousands for the data of [22, 32].

From properties of the set of neuron-stimulus trials, treated as a sample, we deduce estimated response properties for the “universe” of all neurons in particular brain regions and all relevant stimuli. We will formulate the results in terms of the sparsity of individual neurons. Our definition is that the sparsity of a particular neuron is the fraction of stimuli to which it gives a response above some appropriate threshold (e.g., as chosen in [22, 32]). Our aim is to estimate the distribution of sparsity over neurons in a particular brain region. The simplest model, [40], is that all neurons have (approximately) the same sparsity. But, as we will show, such a model is in dramatic disagreement with the data; a more general distribution with widely varying sparsities for different neurons is needed, and we will estimate such a distribution, and show that most neurons in the areas concerned have a sparsity below 10^{-3} .

These results confirm and extend those we made earlier [9]. In particular, the prediction mentioned above is successfully tested, with a quantitative measure of its (excellent) goodness of fit to the newer data. (Minor changes in parameters are needed for the different set of data.)

It has previously been pointed out, notably in [24, 36], that many neurons are unresponsive or even silent, within the limits of experimental measurements over a limited period, as is quantitatively supported by our results. Hence a problem is that reported measurements of responsive neurons can give a very biased picture of the nature of neural coding. Our method provides a tool for both measuring the bias and for compensating for it.

In our discussion section, Sec. VII, we include remarks on the implications of our results for the nature of neural coding of high-level concepts.

II. OUTLINE

After setting up our methods, we apply them to published data from Mormann et al. [22], which presents measurements of the number of neurons as a function of the number of stimuli (out of a total of around 100) to which a particular neuron gives an above-threshold response. The data are for four different areas of the MTL pooled across several patients.

For the distribution of sparsity, we use a model whose

general form has multiple populations of cells, each characterized by a particular sparsity and a fraction of the total neural population. We regard an experiment as using a random sample of neurons and stimuli. The model is in fact a particular kind of mixture model, in statistical terminology, with one component of the mixture for each population. To fit the model to data, an appropriate method is the maximum likelihood method, and it allows us not only to measure the parameters of the model and their uncertainties, but also to evaluate the goodness of fit with the aid of a χ^2 function. We show that the plots given in [22] (numbers of neurons responding a particular number of stimuli) give sufficient statistics for fitting the model, in the sense of standard statistical theory. The much more elaborate statistical treatment used by Waydo et al. [40] is actually unnecessary, and, importantly, did not provide a measure of goodness of fit.

One motivation for using populations of neurons each with a particular value of sparsity arises from work by Attwell and Laughlin [1] and by Lennie [18]. There it is shown that to optimize the energy consumption by neurons transmitting a given amount of information, a particular value of sparsity is preferred, around a few percent. Even if other constraints besides energy consumption are important, the analyses suggest that sparsity is a parameter that could be adjusted (e.g., by evolution) to optimize the performance of a neural system. Therefore it is sensible to propose models in which particular populations of neurons have particular values of sparsity.

Another motivation for trying a multiple-population model is that recent experiments have detected multiple populations of neurons located in the various song-related regions of the brains of zebra finches [16]. These sets of neurons have strikingly different properties of these sets of neurons as regards how often they spike.

We first show that the simplest possible model with one population of neurons, all with the same sparsity, provides an unacceptably bad fit to the data. Such a model is quite often used, for example [40] by the experimental group whose data we fit.

The nature of the deviations between the single-population model and the data will show that at least one more population of very sparsely responding neurons is needed. As an intermediate step we show that a better fit is obtained by adding a population of silent neurons, i.e., of neurons that gave no above threshold responses whatever in the experiment. This provides a greatly improved fit, as expected, but the fit is still poor. Interestingly, the silent neurons are in the majority.

Our main model has two populations of neurons each with a particular sparsity. It has three parameters: the sparsities of the two populations and the relative size of the two populations. We will find greatly improved fits. In the case of the hippocampus, the fit is completely acceptable by the appropriate χ^2 criterion, although in the other areas the fits are poorer, particularly for the PHC. In all cases, we find that at most only about 5% of the neurons have a normal sparsity of a few percent.

The remaining 95% or more of the neurons respond ultra-sparsely, with a sparsity around 0.1%. Thus the vast majority of the neurons are almost silent: they respond on average to much less than one out of the approximately 100 distinct stimuli presented in the experiments. The neurons that are reported as responding are therefore an extremely biased sample of all neurons in the tested regions. Our statistical methods provide a way to quantify this bias and to compensate for it.

Our finding of a large number of silent cells quantitatively supports the conclusions of Shoham, O’Connor and Segev [36] about neural dark matter. It is similar, but more extreme, than a similar conclusion by Olshausen and Field [24] about the (apparent) silence of many neurons in area V1 of the visual cortex.

There are other possible definitions of sparsity and/or selectivity besides the one we chose, and other definitions can give what appear to be dramatically different conclusions. A notable example is the definition of Treves and Rolls [39], who [35] find much larger values of sparsity, around 30%–40%. We will argue that, although the two definitions are equivalent in a certain limit, the high values for Rolls-Treves sparsity can be completely misleading as to the nature of neural coding. We will point out that it is possible that neurons could have a relatively low number of spikes in response to many stimuli but a dramatically higher and readily identifiable response to just a few stimuli. In that case, it can be that the Rolls-Treves sparsity measures mostly the variability of the common low responses, while our sparsity measures the fraction of the selective high responses.

Finally, we will comment on whether our conclusions are robust, on its implications, and on the possibility raised by Waydo et al. [40] that there may be even more apparently silent neurons, so that the true conclusions about ultra-sparsely responding neurons are even more extreme by a substantial factor than what we have fitted.

III. GENERAL MULTI-POPULATION MODEL AND ITS STATISTICAL ANALYSIS

We define the sparsity of a unit or neuron as the fraction of total stimuli that elicit a response from that unit. For our purpose distinct stimuli are distinct visual images of people, objects, etc, such as used in [32]. The threshold for defining a response is set by the experimenters [32]. Only a very small subset of the total possible stimuli are presented in a particular experimental context, and any precise estimates of the sparsity distribution are likely to depend on the circumstances of the experiment.

This definition of sparsity is appropriate where the measured neurons typically have a low firing rate, and occasionally have a much higher firing rate, under specific circumstances. This applies to typical neurons in the kind of data we analyze — see examples in [22, 32].

Related examples that suggest when our definition is appropriate can be found in neural activity in the HVC

area of zebra finches during their song [11, 16]. RA-projecting and X-projecting neurons have occasional high firing rates at consistent points in a bird’s song, with few spikes elsewhere. Our thresholded definition of sparsity would be appropriate (with different values for the RA- and X-projecting neurons, of course). The high responses can be usefully read out, not just by experimentalists, but by other “reader” neurons [7]. In contrast interneurons fire at a high rate during much of the song, but with fairly consistent patterns of various levels of activity. For these, the thresholded, binary definition of sparsity would be less appropriate. It might well be that the interneurons have very low sparsity, since deviations of several standard deviations above the mean firing rate are likely to be rare, according to a visual examination of the figures in [11, 16]. But this would be misleading as to the nature of the interneuron’s firing properties.

In the data that we analyze from [22], units were identified from electrode recordings using spike sorting techniques which cannot always distinguish individual neurons. Thus, the firing patterns reported for some units represent the aggregate firing of multiple neurons rather than for a single neuron. The simplest version of our model ignores this distinction, and assumes that each recorded unit consists of only a single neuron. But, as we will explain in Sec. VI, the general principles of our methods apply perfectly well at the unit level. We will show how to transform from a neural-level model to a unit-level model, and we will see how to interpret numerical results of fits at the unit level in terms of single neuron properties. This will result in no change in our qualitative results, but a strengthening of our conclusions about the presence of a large number of very sparsely responding neurons.

A. Model Definition

In the data we analyze, the unit firing patterns are treated in a binary fashion. The threshold for a response is defined by the experimentalists [22, 32]. We assume:

- The sparsity of each neuron remains constant over the course of the experiment.
- The recorded neurons are statistically independent of each other.
- The neurons are partitioned into distinct populations, each with fractional abundance, f_i , where i labels the population.
- All neurons in population i have the same sparsity, α_i .

The statistical independence of the recorded neurons was verified experimentally [32].

Our ultimate goal is find an appropriate set of populations, with their fractional abundances and sparsities. However, as will become apparent later, data has limited

ability to distinguish populations with sparsities that are close to each other: in that situation the effect is close to that of a single population with a single averaged sparsity. In contrast, the data do provide the ability to distinguish populations of widely different sparsities. So our practical goal will be to find the simplest model that is consistent with reported data; the model is thus meant only to be a useful approximation to reality.

In this paper, we will start from a very simple model with one population of neurons, and elaborate it in two stages. This will give three models:

1. Single-population model: All neurons have the same sparsity, α . This model has one parameter.
2. Two-population model, with one population silent: The active population has sparsity α_D and abundance f_D , while the other population is silent with $\alpha_S = 0$, and abundance $1 - f_D$. This model has two parameters.
3. Full two-population model: Two active populations are present, one with parameters α_D and f_D , and one ultra-sparse population with parameters α_{US} and $f_{US} = 1 - f_D$. This model has three parameters. The labeling of the populations is defined by choosing $\alpha_{US} < \alpha_D$.

For each model, we first produce the best fit to the data in [22], by using a maximum likelihood estimates (MLE) for the parameters [19]. We will do this for each of the four regions of the MTL for which data is reported. Then we test the goodness of the fit by using a χ^2 analysis.

B. Mathematical characterization of data and model

To implement the MLE of the parameters, we first derive the likelihood function for the model. This is defined [19] as the probability of the data given the model and its parameters.

Given that the neurons are treated as binary (responsive or not responsive), the data from an experiment in which N neurons are recorded during the presentation of S stimuli can be fully represented by a collection of NS Bernoulli random variables, X_{js}

$$X_{js} = \begin{cases} 1, & \text{if neuron } j \text{ responds to stimulus } s, \\ 0, & \text{if neuron } j \text{ does not respond to } s. \end{cases} \quad (1)$$

Our model in its general form has M populations, with population i having fractional abundance f_i and sparsity α_i . The fractional abundances add to unity:

$$\sum_{i=1}^M f_i = 1, \quad (2)$$

so that there are $2M - 1$ model parameters: the sparsity of each population, the fractional abundance of each population, but minus one for the constraint (2).

If we knew the population i_j to which a neuron j belongs, then the probability distribution of X_{js} would be²

$$\begin{aligned} \text{Prob}(X_{js}=x_{js} \mid \alpha_{i_j}) &= \begin{cases} \alpha_{i_j}, & \text{if } x_{js} = 1, \\ 1 - \alpha_{i_j}, & \text{if } x_{js} = 0 \end{cases} \\ &= \alpha_{i_j}^{x_{js}} (1 - \alpha_{i_j})^{1-x_{js}}. \end{aligned} \quad (3)$$

Then the probability of a particular outcome in the showing of S stimuli to the whole set of neurons is:

$$\begin{aligned} \text{Prob}(\{X_{js} = x_{js}\} \mid \{\alpha_{i_j}\}) &= \prod_{j,s} \text{Prob}(X_{js}=x_{js} \mid \alpha_{i_j}) \\ &= \prod_j \left[\alpha_{i_j}^{\sum_{s=1}^S x_{js}} (1 - \alpha_{i_j})^{S - \sum_{s=1}^S x_{js}} \right]. \end{aligned} \quad (4)$$

Here $\{X_{js} = x_{js}\}$ and $\{\alpha_{i_j}\}$ denote the whole array of the quantities notated.

It is now convenient to define two sets of auxiliary random variables. One is the number of responses that a particular neuron makes:

$$K_j = \sum_{\text{stimuli } s} X_{js}. \quad (5)$$

The second is the number of neurons N_k that give k responses to the stimuli:

$$N_k = \sum_{\text{neurons } j} \delta_{k, K_j}, \quad (6)$$

where as usual, the Kronecker delta $\delta_{\alpha\beta}$ obeys $\delta_{\alpha\beta} = 1$ if $\alpha = \beta$ and $\delta_{\alpha\beta} = 0$ otherwise.

We can then write the probability of the data (given the set of α_{i_j}) in terms of the values k_j of the random variables K_j alone:

$$\text{Prob}(\{X_{js} = x_{js}\} \mid \{\alpha_{i_j}\}) = \prod_j \left[\alpha_{i_j}^{k_j} (1 - \alpha_{i_j})^{S - k_j} \right]. \quad (7)$$

But we do not know the values of each neuron's sparsity, so the probability of the data given the model parameters is given by summing over the possible sparsity values weighted by their probabilities:

$$\begin{aligned} \text{Prob}(\{X_{js} = x_{js}\} \mid \{\alpha_i, f_i\}) \\ = \prod_{j=1}^N \left[\sum_{i=1}^M f_i \alpha_i^{k_j} (1 - \alpha_i)^{S - k_j} \right]. \end{aligned} \quad (8)$$

² Here and elsewhere, we use a notational convention that is common in the statistical literature: X_{js} with an upper case X denotes a random variable in the technical statistical sense, while the corresponding symbol x_{js} with a lower-case name x denotes a numerical value of the random variable that results from a particular set of experimental observations.

This depends only on the values of the random variables K_j , and not on any more detailed properties of the data. That is, the values of K_j are sufficient statistics for fitting the model.

Therefore it is useful to compute the probabilities for the K_j . First, for one neuron of given sparsity α , the probability of k responses, in the presentation of S random images, is the binomial distribution:

$$P(K = k | \alpha) = \binom{S}{k} \alpha^k (1 - \alpha)^{S-k}. \quad (9)$$

Here the factor $\binom{S}{k} = S!/(k!(S-k)!)$ counts the number of ways of getting k responses to S stimuli. The distribution (9) has mean αS and standard deviation $\sqrt{\alpha(1-\alpha)S}$, which is approximated by $\sqrt{\alpha S}$ for the actual situation of $\alpha \ll 1$. The ratio of standard deviation to mean is $\sqrt{(1-\alpha)/(\alpha S)} \simeq 1/\sqrt{\alpha S}$, which goes to zero as $S \rightarrow \infty$. If we plot the distribution of k/S , i.e., the distribution of the fractional response rate, this can be regarded as a smearing of the delta function $\delta(k/S - \alpha)$.

In the model, there are M distinct neuronal populations, each with sparsity α_i and fractional abundance f_i . If the population to which the neuron belongs is unknown, then its probability of responding to k out of S stimuli is

$$\begin{aligned} \epsilon_k \equiv P(K=k) &= \sum_i f_i P(K=k | \alpha_i) \\ &= \sum_{i=1}^M f_i \binom{S}{k} \alpha_i^k (1 - \alpha_i)^{S-k}. \end{aligned} \quad (10)$$

With the aid of Eq. (2), one can check that the probabilities in Eq. (10) correctly sum to unity: $\sum_{k=0}^S \epsilon_k = 1$.

We already know that the K_j are sufficient statistics for fitting the model to the data. So we need the probabilities for the set of K_j :

$$\text{Prob} \left(\bigwedge_{j=1}^N K_j = k_j \right) = \prod_{j=1}^N \epsilon_{k_j} = \prod_{k=0}^S \epsilon_k^{n_k}, \quad (11)$$

where “ \wedge ” denotes “and”. In the last part of this equation, we have simply counted the number of neurons with a given value of k , for every possible value of k . Since the result depends only on the values of n_k , these themselves form a set of sufficient statistics for fitting the model to the data. Ref. [22] provided results for these numbers, and no further information on the raw experimental data is needed to fit the parameters of the model; examination of the other quantities used in the work of Waydo et al. [40] is unnecessary.

C. Likelihood and its analysis

Since the random variables N_k are sufficient statistics, we need the probabilities for them. From these we obtain the likelihood function that we will use for fitting

the model to the data. It is obtained from Eq. (11) by counting the number of different arrays of K_j that given a given set of N_k s. We then get

$$\begin{aligned} \mathcal{L}(\{\alpha_i, f_i\} | \text{Data}) &\equiv \text{Prob}(\{N_k = n_k\} | \{\alpha_i, f_i\}) \\ &= \frac{N!}{\prod_{k=0}^S n_k!} \prod_{k=0}^S \epsilon_k^{n_k}. \end{aligned} \quad (12)$$

In this likelihood function, the dependence on the model parameters, $\{\alpha_i, f_i\}$, is contained in the ϵ_k .

Note that in making the transformation from a distribution over X_{js} to K_j and then to N_k , we have greatly reduced the number of data items to be considered, from NS to N (the number of neurons) to S (the number of stimuli). Moreover, as can be seen from the data in [22], only the first few N_k are nonzero in reality, at least to a good approximation.

To estimate the values of the parameters of the model, we use the maximum-likelihood method, as is appropriate for this situation.

The methods we use are, in fact, almost identical to long-established methods [2, 19] that are regularly used for analyzing data from scattering experiments in high energy physics (and more generally, scattering experiments in physics). This close similarity arises because both in the scattering experiments and in the neural data, we have a large number of independent trials, and the probability of a non-trivial outcome is small. A non-trivial outcome in the physics case is a scattering event between pairs of particles in the beams in an experiment, while in the neural case it is an above-threshold response by a particular neuron to a particular stimulus. The physics analog of the neural N_k is the number of scattering events in a certain bin of kinematics.

Although our methods are informed by those used in the physics case, we will provide a self-contained treatment appropriate to the neural case. An important tool we will take over from high-energy physics is an appropriately defined χ^2 function that is closely related to the logarithm of the likelihood function. Minimization of a suitably defined [2, 12] χ^2 is equivalent to maximizing likelihood. The minimum value of χ^2 provides a very convenient measure of goodness of fit, to assess how consistent the data are with the model. The shape of the χ^2 function near the minimum can also be used to estimate the uncertainties on the fitted values of the parameters of the model, and also the correlations in the uncertainties.

The ϵ_k are subject to the normalization constraint

$$\sum_{k=0}^S \epsilon_k = 1, \quad (13)$$

while the n_k are constrained by

$$\sum_{k=0}^S n_k = N. \quad (14)$$

The maximum likelihood method finds the best fit to the data by maximizing $\mathcal{L}(\{\alpha_i, f_i\})$ with respect to the parameters f_i and α_i .

The data show that the probability of a neural response is much less than one. Thus we can usefully make approximations appropriate for the situation that $\epsilon_k \ll 1$ and $n_k \ll N$ for $k \geq 1$. Hence ϵ_0 is close to unity, while n_0 is less than N only by a small fraction. Under these approximations, the likelihood function simplifies to:

$$\mathcal{L} \approx \prod_{k=1}^S e^{-N\epsilon_k} \frac{(N\epsilon_k)^{n_k}}{n_k!}, \quad (15)$$

i.e., a product of Poisson distributions for each of the *non-zero* k values. A derivation is given in the Appendix.

D. Error analysis

Suppose that we have estimated the best fit parameters by maximizing likelihood with respect to the parameters $\{\alpha_i, f_i\}$. Then taking the likelihood function to be approximately Gaussian in the vicinity of its maximum, we can estimate the confidence intervals and correlations of the model parameters [19] from the diagonal terms of the covariance matrix, defined by:

$$\text{cov}(\theta_i, \theta_j) = - (H^{-1})_{ij}, \quad (16)$$

where the Hessian matrix is

$$H_{ij} = \frac{\partial^2}{\partial \theta_i \partial \theta_j} \ln \mathcal{L}. \quad (17)$$

The diagonal terms yield the parameter variances, $\text{cov}(\theta_i, \theta_i) = \sigma_i^2$. Correlations between model parameters, ρ_{ij} , can be determined from the off-diagonal elements of Eq. (16),

$$\rho_{ij} = \frac{\text{cov}(\theta_i, \theta_j)}{\sigma_i \sigma_j}. \quad (18)$$

Two important properties of a Poisson distribution $e^{-N\epsilon_k} (N\epsilon_k)^{n_k} / n_k!$ are its mean and standard deviation

$$\langle N_k \rangle = N\epsilon_k, \quad \text{s.d.}(N_k) = \sqrt{N\epsilon_k}. \quad (19)$$

Thus we can characterize the typical values of n_k by $n_k = N\epsilon_k \pm \sqrt{N\epsilon_k}$.

We will assess goodness of fit by using the following χ^2 function:

$$\chi^2(k_{\max}; n_1, n_2, \dots) = \sum_{k=1}^{k_{\max}} \frac{(n_k - N\epsilon_k)^2}{N\epsilon_k}. \quad (20)$$

This corresponds to $-2 \ln \mathcal{L}$, to within an additive constant, when the Poisson distributions are replaced by Gaussian approximations near their peak. But this approximation is only suitable when $N\epsilon_k$ is reasonably

much larger than one. So, in Eq. (20), we truncated the sum over k to $k \leq k_{\max}$. The restriction should be those values of k such that the expected value of n_k is bigger than one or two, i.e., where there are noticeable neural responses. Beyond k_{\max} , there are very few neural responses, and therefore little information for fitting the parameters of the model.

After we have performed a maximum-likelihood estimate of the parameters of the model, statistical theory [19] predicts a mean and standard deviation for χ^2 :

$$\chi^2 = N_{\text{dof}} \pm \sqrt{2N_{\text{dof}}}. \quad (21)$$

where the number of degrees of freedom, N_{dof} , is the number of data values used (i.e., the number of values of k in the truncated sum) minus the number of parameters fitted (which will be 1, 2 or 3, in the particular implementations of the model that we use). If the value of χ^2 falls much outside this range, that indicates that the model does not agree with the data.

IV. MULTI-UNIT CONSIDERATIONS

The preceding analysis assumes that the recorded units all consist of a single neuron. However, only a fraction of the recorded units contain a single neuron while the rest are composed of several neurons.

We now show that given our general multipopulation model at the neuron level, a version of the model also applies at the unit level. That is, each unit has a sparsity, which can be calculated as a function of the sparsities of its constituent neurons, and there are populations of units with different values of sparsity.

This is the general picture. Some simplifications and useful approximations can be made in the application to real data, as we will see in Sec. VI.

Suppose first that a particular unit consists of R neurons of known sparsities. Let $r = 1, \dots, R$ label the neurons, and let α_{i_r} be the sparsity of neuron r . The unit's sparsity, i.e., the probability that the unit responds to a presented stimulus is given by:

$$\alpha' \equiv \text{Prob}(\text{response} \mid R, \alpha_{i_1}, \dots, \alpha_{i_R}) = 1 - \prod_{r=1}^R (1 - \alpha_{i_r}). \quad (22)$$

Then the probability that the unit responds to k of S stimuli given R and the α_{i_r} is a binomial distribution:

$$\text{Prob}(K = k \mid R, \alpha_{i_1}, \dots, \alpha_{i_R}) = \binom{S}{k} (\alpha')^k (1 - \alpha')^{S-k}. \quad (23)$$

So far, we have assumed that R and the sparsities α_{i_R} are known. Next, we assess the unit sparseness in terms of the probability distribution of the neural sparsities. Let $\epsilon_{k,R}^{\text{unit}}$ be the total probability that the unit responds to k stimuli given the number R of neurons in the unit.

Then $\epsilon_{k,R}^{\text{unit}}$ is given by summing Eq. (23) over the distributions of α_{i_r} . In the M -population model for the neurons,

$$\begin{aligned} \epsilon_{k,R}^{\text{unit}} &= \int d\alpha_{i_1} \dots d\alpha_{i_R} \text{Prob}(K = k \mid R, \alpha_{i_1}, \dots, \alpha_{i_R}) \\ &\quad \times \text{Prob}(\alpha_{i_1}, \dots, \alpha_{i_R}) \\ &= \sum_{i_1=1}^M \dots \sum_{i_R=1}^M f_{i_1} f_{i_2} \dots f_{i_R} \binom{S}{k} (\alpha')^k (1 - \alpha')^{S-k}, \end{aligned} \quad (24)$$

with α' given by Eq. (22). This is in fact a version of the original multi-population model, whose ϵ_k is given in Eq. (10), with a more complicated labeling of the populations.

If the number of neurons in the unit, R , is sampled from a distribution, $g(R)$, then the total probability that a unit responds to k of S stimuli, ϵ_k^{unit} is given by

$$\epsilon_k^{\text{unit}} = \sum_{R=1}^{\infty} g(R) \epsilon_{k,R}^{\text{unit}}. \quad (25)$$

Again, this is a case of a multi-population model. Eq. (25) is then substituted for ϵ_k in the likelihood function, Eq. (15), and the rest of the analysis proceeds in an identical fashion as with the single-neuron unit model.

The combination of Eqs. (24) and (25) shows that from the populations at the neural level, with their abundances and sparsities, we obtain a (larger) set of populations at the unit level: In all cases, Eqs. (10), (24), and (25), ϵ_k is a linear combination of binomial distributions. Although the structure of the populations appears complicated, considerable approximate simplifications will become apparent when we fit data.

V. FITS TO DATA

The data [22] being analyzed come from recordings of single neuron activity in four regions of the human MTL, the hippocampus (Hipp), the entorhinal cortex (EC), the amygdala (Amy), and the parahippocampal cortex (PHC). Altogether, 1194 neurons/units were detected in the hippocampus, 844 in the entorhinal cortex, 947 in the amygdala, and 293 in the parahippocampal cortex, accumulated over patients. During the experiment, the patients were shown a randomized sequence of images of famous individuals, landmarks, animals, and objects. For each session, the patients were shown on average 97 images, each of which was presented six times during the random sequence. Histograms of the number of responses per unit for neurons in the four MTL regions were then produced. The values are given in Table I, which we read from graphs in Fig. 3 of [22].

In this section we show the results of fits to the data with the three model implementations of our general scheme, that we summarized in Sec. III A. We start with

a simple model with one population of neurons with a single sparsity. Analyzing the disagreement between data and model leads us to first to add a population of completely silent neurons, and then to allow the second population a non-zero sparsity. We fit the parameter(s) of each model separately for each of the brain regions for which data were given. In Table II, we tabulate the numerical results of the fits of each model in each region. In Figs. 1–4, we show the results graphically; each figure shows the results of the three fits for a single region.

A. One-Population Model

First, we attempt to fit the data in the four regions assuming only one population of neurons with sparsity α . In this case, Eq. (10) becomes:

$$\epsilon_k = \binom{S}{k} \alpha^k (1 - \alpha)^{S-k}. \quad (26)$$

Substituting this into the likelihood function, and maximizing with respect to α , yields a maximum likelihood estimate (MLE) for the sparsity. For this and the other fits, the maximization was performed numerically in Mathematica, and we used the exact formula (12) for the likelihood, without any approximation such as (15).

The parameters of the fits are shown numerically in Table II(a). In the top row of each of Figs. 1–4, the data for each region are compared with the expectation values of the response counts N_k

$$\langle N_k \rangle = N \epsilon_k. \quad (27)$$

The error bars in the plots are the one-standard-deviation variations that the model predicts for the N_k over repetitions of the whole experiment.

We assess the goodness of fit of the model to the data by the χ^2 test, with χ^2 defined in Eq. (20). The enormous values of χ^2 — see Table II(a) — show that the fits are extremely bad, given the expected range, Eq. (21).

The nature of the bad fit is seen in the plots in the top row of each of Figs. 1–4. Because the value of n_0 , the number of non-responding neurons, is much larger than for the other n_k , we show two versions of the plot. The right-hand plots have the $k = 0$ bin omitted and have a changed vertical scale, to better exhibit the other bins.

The data considerably exceed the best fit in the $k = 0$ bin in all 4 regions, but undershoot the fit in the other bins. We have a choice. If the sparsity is large enough to give a sufficient number of cells that respond to multiple stimuli, then, compared with data, too few cells are non-responsive. If instead, the sparsity is low enough to reproduce the number of non-responsive cells (i.e., n_0), then there is much too small a probability for multiple responses. In either case, the model cannot reproduce all the data.

	n_0	n_1	n_2	n_3	n_4	n_5	n_6	n_7	n_8	n_9	n_{10}	n_{11}	n_{12}	n_{13}	n_{14}
Hipp	1019	113	30	17	7	4	1	2	0	0	0	0	1	0	0
EC	761	45	15	9	4	8	0	0	1	0	0	0	0	1	0
Amy	842	61	17	15	3	3	1	0	1	1	0	0	0	1	2
PHC	244	13	11	7	3	0	4	1	2	4	3	0	1	0	0

TABLE I: Number of neurons n_k responding to k images as reported by [22] in four MTL regions.

	Hipp	EC	Amy	PHC
α	$(2.6 \pm 0.1) \times 10^{-3}$	$(2.2 \pm 0.2) \times 10^{-3}$	$(2.5 \pm 0.2) \times 10^{-3}$	$(6.8 \pm 0.5) \times 10^{-3}$
$\chi^2(5)$	5.1×10^2	4.8×10^2	3.4×10^2	2.5×10^2

(a) One-population model.

	Hipp	EC	Amy	PHC
α_D	$(1.3 \pm 0.1) \times 10^{-2}$	$(1.9 \pm 0.2) \times 10^{-2}$	$(1.9 \pm 0.1) \times 10^{-2}$	$(4.0 \pm 0.3) \times 10^{-2}$
f_D	0.21 ± 0.02	0.11 ± 0.01	0.13 ± 0.01	0.17 ± 0.02
$\chi^2(5)$	20	19	33	29

(b) Two-population model, with one population being totally silent.

	Hipp	EC	Amy	PHC
α_D	$(2.6 \pm 0.3) \times 10^{-2}$	$(3.2 \pm 0.4) \times 10^{-2}$	$(3.8 \pm 0.4) \times 10^{-2}$	$(5.1 \pm 0.4) \times 10^{-2}$
f_D	0.06 ± 0.01	0.05 ± 0.01	0.05 ± 0.01	0.12 ± 0.02
α_{US}	$(1.0 \pm 0.1) \times 10^{-3}$	$(5.4 \pm 1.0) \times 10^{-4}$	$(7.4 \pm 1.1) \times 10^{-4}$	$(5.8 \pm 2.0) \times 10^{-4}$
f_{US}	0.94 ± 0.01	0.95 ± 0.01	0.95 ± 0.01	0.88 ± 0.02
$\chi^2(5)$	2.3	3.7	14.3	20
$\chi^2(10)$	5.7	10.5	19.9	36

(c) Full two-population model.

TABLE II: Results of the fits of the three models. For each model, we give the values and uncertainties of the model's parameters for each brain region, and we give the χ^2 measuring the goodness of fit.

B. One Active Population, One Silent Population Model

A simple and natural improvement to the model is to add a population of completely silent neurons that do not respond to any of the stimuli used — cf. [36]. That is, we make a 2-population model with one active and one silent population of neurons. The silent population has sparsity zero. For the active population, let α_D be its sparsity, and let f_D be its fractional abundance. In this case, Eq. (10) becomes

$$\epsilon_k = f_D \binom{S}{k} \alpha_D^k (1 - \alpha_D)^{S-k}, \quad (28)$$

for $k \geq 1$.

The results of a maximum-likelihood fit are shown numerically in Table II(b), and graphically in the middle row of each of Figs. 1–4. The fits are much improved, but the χ^2 values are still substantially too large for a

good fit. Notice how the silent population contains by far the majority of the neurons in all four regions.

The pattern of deviations between data and model is now an excess for the data in the $k = 1$ bins and a deficit at higher k . That is, the number of cells responding exactly once is substantially higher compared with the extrapolation of the numbers of cells with multiple responses. This indicates that a better model would be to replace the silent neural population by a slightly active population. To fit the data, this population must have a very small sparsity, so that it predominantly gives contributions to the $k = 0$ and $k = 1$ bins only.

C. Two-Population Model

Therefore our final model uses two active populations each with a particular sparsity. One population we call the distributed population, with a sparsity α_D and fractional abundance f_D . The other population we call the

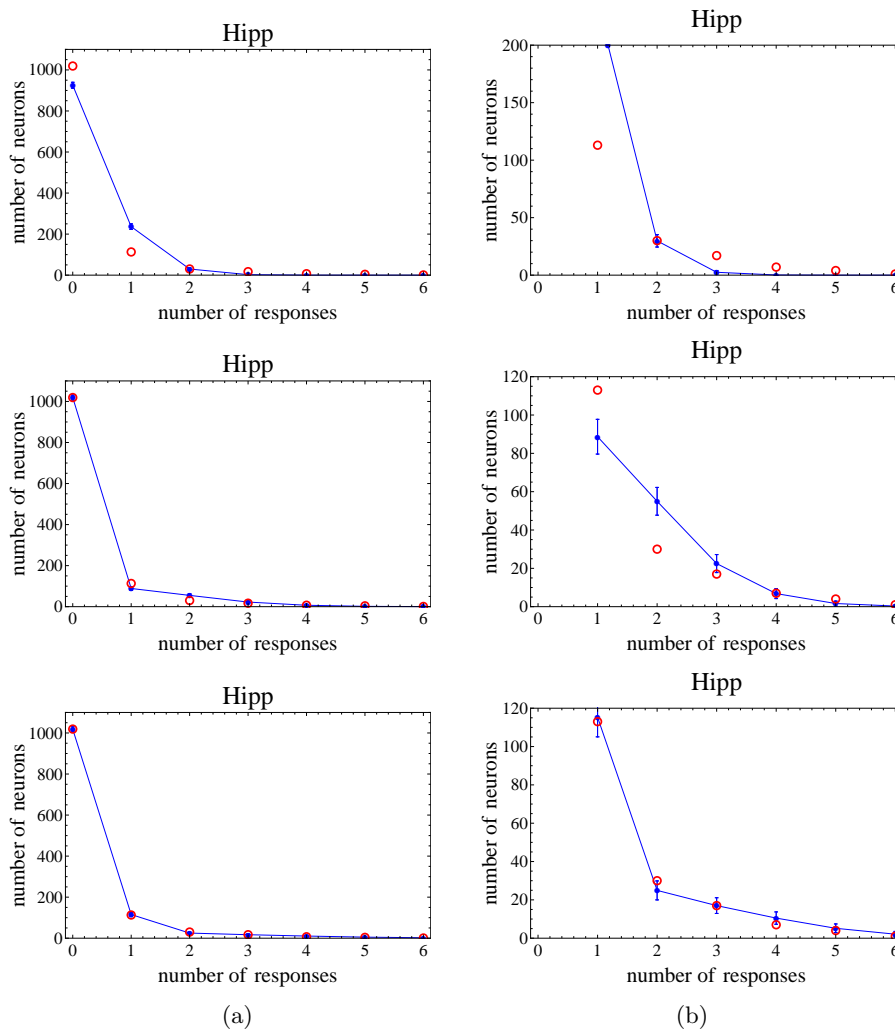


FIG. 1: Comparison of data from the hippocampus with fits for the number of neurons n_k that respond to k stimuli, for each of the three models. The red circles indicate the experimental values and blue dots connected by lines indicate the model predictions for the expectation values of n_k . The blue error bars indicate the model's prediction for the one-standard-deviation variation of experimental results on repetition of the experiment. The top plots are the fits from the one-population model. The middle plots are fits from the model with one active and one silent population. The bottom fits are for the model with two active populations. The left-hand plots are with the zero-response bin included, and the right-hand plots are without them, to show more clearly the other bins.

ultra-sparse population with sparsity α_{US} . The fractional abundance of the ultra-sparse population is $f_{US} = 1 - f_D$. Then Eq. (10) becomes

$$\epsilon_k = (1 - f_D) \binom{S}{k} \alpha_{US}^k (1 - \alpha_{US})^{S-k} + f_D \binom{S}{k} \alpha_D^k (1 - \alpha_D)^{S-k}. \quad (29)$$

The labeling of the populations is defined by $\alpha_{US} < \alpha_D$.

The results of a maximum-likelihood fit are shown numerically in Table II(c), and graphically in the bottom row of each of Figs. 1–4. The fits are much improved. For both the hippocampus and the entorhinal cortex, we have good fits, with the model being consistent with the data. The fit in the amygdala is less reliable and the

model poorly fits the data in the parahippocampal cortex. In all cases, the ultra-sparse population is in the vast majority, around 90% or more, while at the same time having a very small sparsity, 10^{-3} or smaller. Thus each neuron in the ultra-sparse population responds on average to at most about 0.1 stimuli in a session. We only see the effects of the ultra-sparse population because the data are from a large number of neurons. In contrast, the remaining few percent of neurons in the other population typically respond to several stimuli in each session.

For the parahippocampal cortex (PHC), a different or more general model is clearly needed. We observe that the functionality of the PHC is much different than that of the hippocampus and the entorhinal cortex, so it is not surprising that its neural coding properties should

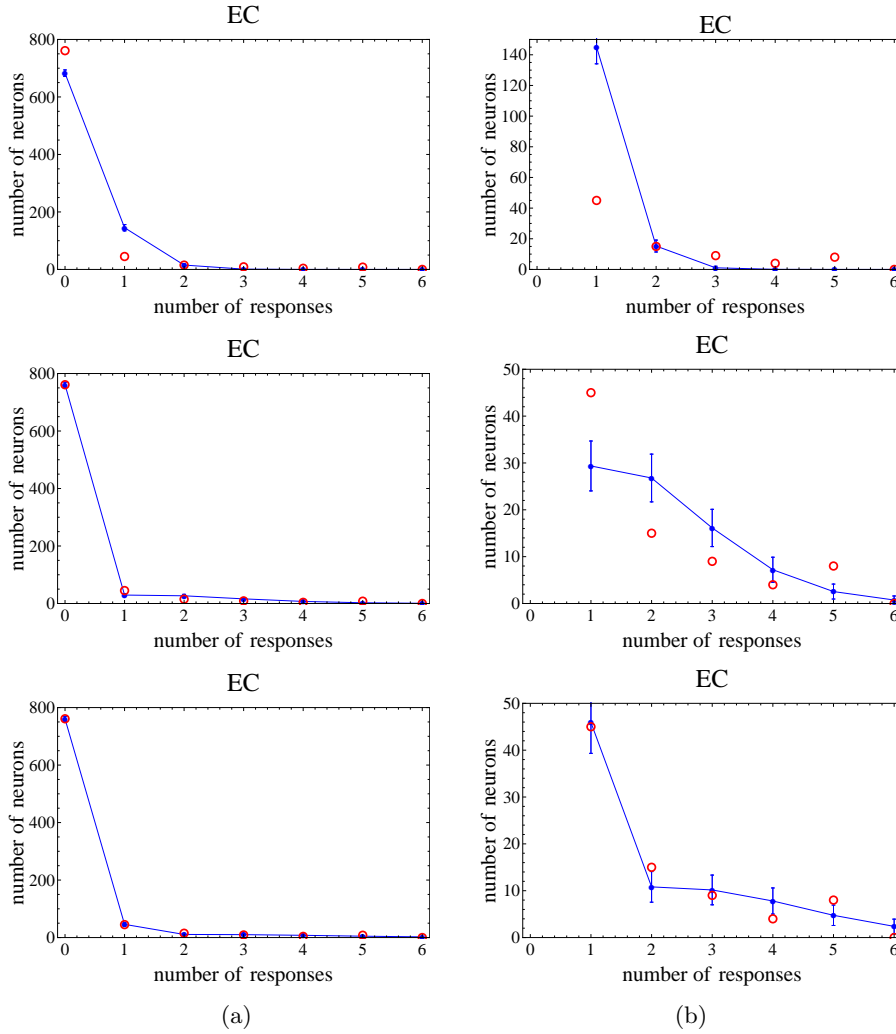


FIG. 2: The same as Fig. 1, but for the entorhinal cortex.

be different. The hippocampus is the classical locus of episodic memory storage, and the entorhinal cortex is its main source of input (and output).

An alternative view of the fit is shown in Fig. 5. Here we show how the neural responses are predicted by the model to arise from the different populations. The bottom parts of the bars, shaded gray, show the expectation values for the part of N_k coming from above-threshold responses by neurons in the D population. Stacked above these are open bars, showing the contribution from the US population. In the bins with more than one response, i.e., $k \geq 2$, almost all the responses are from the D population, with only a small contamination from the ultra-sparse population, primarily at $k = 2$. In contrast, in the $k = 1$ bin, there is a relatively small fraction of responses from the D population, from the tail of a distribution with its peak at several responses. The majority of the $k = 1$ bin is from the ultra-sparse population. However, this represents only the tip of the iceberg, so to speak. The vast majority of the ultra-sparse neurons give no above-threshold responses; they appear in the $k = 0$ bin,

which is much too tall to be shown in Fig. 5.

The sparsity and fraction for the D population can be determined from the $k \geq 2$ bins, i.e., with the exclusion of the $k = 1$ bin. There are several bins involved, so the shape of the distribution of N_k from a single sparsity fit is confirmed, as can be seen from the lowest plots in the right-hand column of Figs. 1–4, certainly for the HC and EC regions. Extrapolating the fit for the D population to the $k = 1$ falls far short of the data, by a factor of at least 5. This then determines that there is an ultra-sparse population, whose average sparsity is determined to a good approximation by the excess in the $k = 1$ bin relative to the total number of non-D neurons:

$$\alpha_{\text{US}} \simeq \frac{N_1(\text{excess above extrapolation})}{N(1 - f_D)S}. \quad (30)$$

Our actual best fit allows for the contamination of the bins of higher k by the ultra-sparse population. The existence and size of the ultra-sparse population is determined by the large excess of the measured value of N_1 compared with the extrapolation from the bins of larger

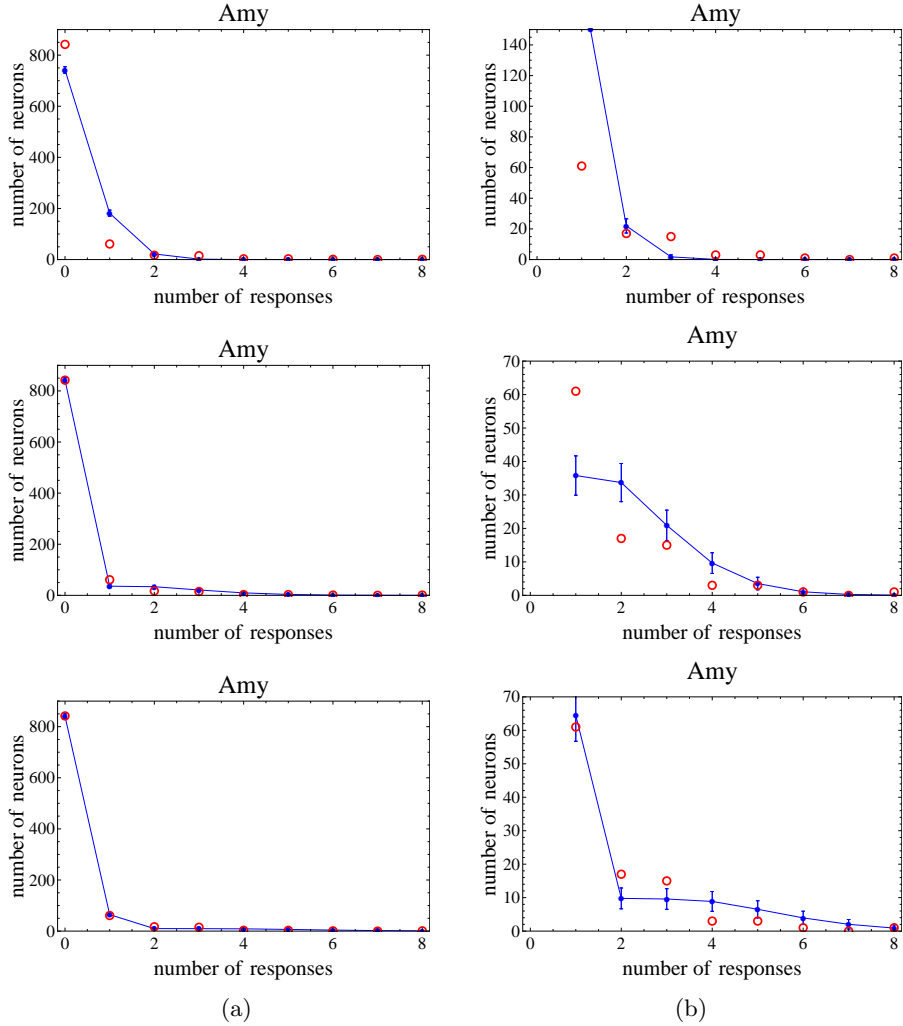


FIG. 3: The same as Fig. 1, but for the amygdala.

k , whose relative sizes correspond to a sparsity of a few per cent.

D. Uncertainties and correlations in fitted parameters

We computed uncertainties and correlations in the fitted values of the models' parameters by the method described in Sec. III D. The uncertainties are reported in Table II. Correlations between the three parameters of the full two-population model were calculated using Eq. (18), and are shown in Table III.

E. Comparisons of the three versions of the model

We can see that the results of fitting the first single-population model with its single sparsity were intermediate sparsities compromising between the extremes of the two populations in the full model. The single-population

	$\rho_{\alpha_{US}, \alpha_D}$	ρ_{α_{US}, f_D}	ρ_{α_D, f_D}
Hipp	0.46	-0.52	-0.62
EC	0.34	-0.33	-0.41
Amy	0.33	-0.31	-0.37
PHC	0.30	-0.23	-0.19

TABLE III: Correlations between parameters of the two-active population model, assuming all recorded units are comprised of a single neuron. The presence of units consisting of two neurons did not affect the correlations between parameters to within two significant digits.

model therefore incorrectly represents the actual neural sparsity. Our fitted values of sparsity in Table II(a) roughly match those found by Waydo et al. [40] in their fit of a pure one-population model to similar data.

In the second model, with a set of exactly silent neurons, the fit for the responsive neurons is qualitatively similar to the D neurons in the full model: a sparsity of a percent to a few percent and a minority abundance.

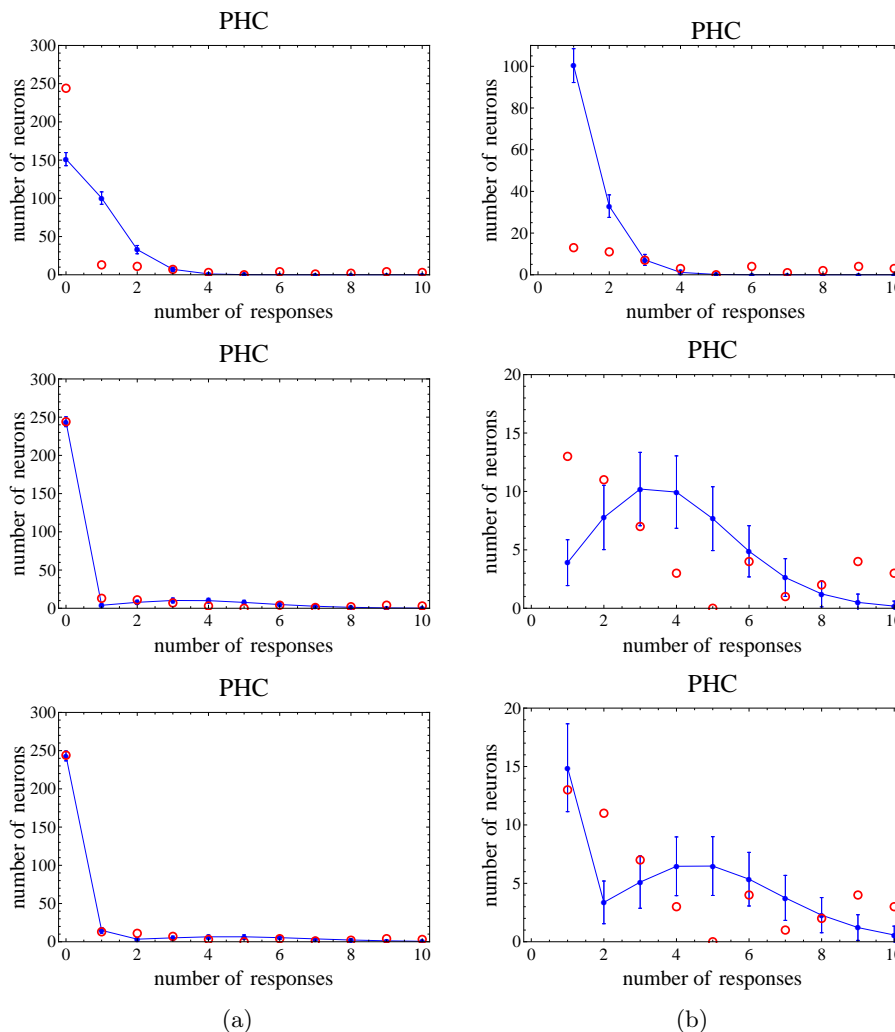


FIG. 4: The same as Fig. 1, but for the parahippocampal cortex.

Relative to the full model, the value for the active population's sparsity is still biased downwards, while its fractional abundance is biased upwards; these properties give a compromise between the effects of the two populations of neurons in the full model.

Merely introducing extra parameters increases the goodness of fit, but only by an expected decrease of one unit in χ^2 per parameter, as in Eq. (21). So the improved fits from adding an extra population are highly significant. In all cases, the p -values for the poor fits for the first two models are well below 0.001, from standard plots or tables for the χ^2 distribution.

VI. MULTI-NEURON UNIT RESULTS

The results presented thus far have been under the assumption that all recorded units are composed of a single neuron. However, it is known that some units are in fact composed of multiple neurons [22, 32]. To gain an idea of the effect of such multiunits on our fits and

of our conclusions about neural properties, we apply the general analysis from Sec. IV.

A. Implementation of multi-unit model

To fit the data taking into consideration the presence of multi-neuron units, we must maximize the likelihood function, Eq. (15) after replacing the ϵ_k , with the function ϵ_k^{unit} , Eq. (25). In the case of the model with two populations at the neural level, i.e., with $M = 2$, Eq. (24) becomes

$$\epsilon_{k,R}^{\text{unit}} = \sum_{l=0}^R \binom{R}{l} f_D^l f_{US}^{R-l} \binom{S}{k} (\alpha'_{l,R})^k (1 - \alpha'_{l,R})^{S-k}, \quad (31)$$

where

$$\alpha'_{l,R} = 1 - (1 - \alpha_D)^l (1 - \alpha_{US})^{R-l}, \quad (32)$$

and, of course $f_{US} = 1 - f_D$. Here l and $R - l$ are the numbers of neurons in the unit that are in the D and US

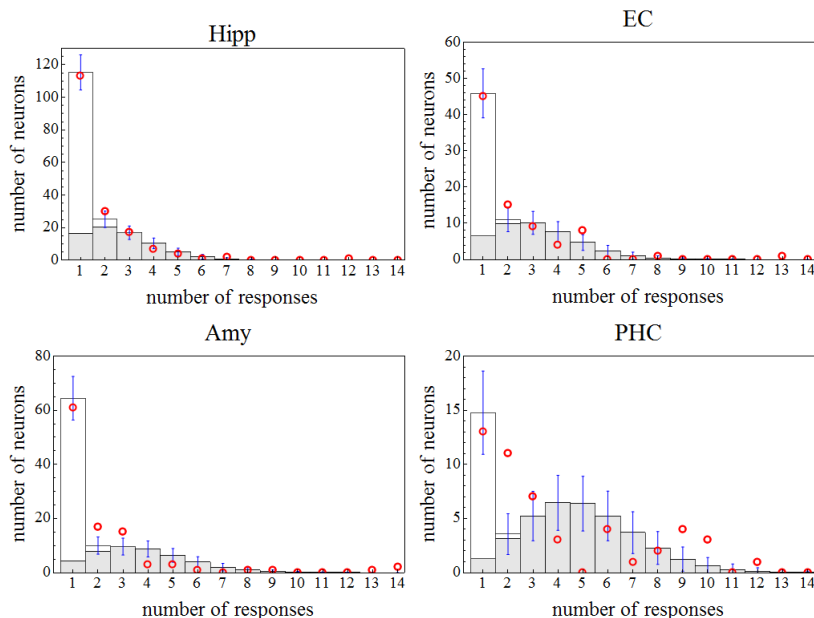


FIG. 5: Plots of neuron responses predicted by the three-parameter maximum-likelihood fits to data in four regions of the MTL. The plots are of number of neurons as a function of number of responses. The shaded bars represent neurons in the almost-silent population while the open bars correspond to the distributed population. The red circles indicate the experimental values.

populations. The result is that at the unit level, we have multiple populations, each with its distinct sparsity. The different populations correspond to the different terms in the summation in Eq. (31).

For units with $R = 1$, these just correspond to the original two neural populations. For $R = 2$, there are three populations. One of these, the most common case, is where both neurons in the unit are US neurons, giving a sparsity $1 - (1 - \alpha_{US})^2 \simeq 2\alpha_{US}$, twice that of a single neuron. The second most common situation is where one neuron is in each neural population; these units have sparsity $1 - (1 - \alpha_D)(1 - \alpha_{US}) \simeq \alpha_D + \alpha_{US} \simeq \alpha_D$, where the last approximation follows from the fact, confirmed by our detailed fit later, that α_{US} is much less than α_D . The third population, a small fraction f_D^2 of the units, has a larger sparsity $1 - (1 - \alpha_D)^2 \simeq 2\alpha_D$.

If only single-neuron and double-neuron units existed, i.e., if only $R = 1$ and $R = 2$ occur, then the total number of populations at the unit level would be 5, and these would appear in the formula (25) for ϵ_k^{unit} . If larger multi-units occur, there are even more populations of units, each with its particular sparsity. This seems like a very complicated situation, but provides no issue of principle in the MLE of the parameters of the populations at the neural level, except that there is little data about the exact distribution of the number of neurons in a unit.

However, as we will see in more detail shortly, considerable simplifications occur because the vast majority of neurons are extremely sparsely firing. This property is reflected at the unit level, and we will see that from a 2-population model at the neural level, the unit-level data are reasonably accurately given by a 2-population

model at the unit level. This justifies a posteriori the success of a 2-population model applied to unit level data, and one can see how to relate properties of the neural populations to properties of the unit populations. The reasons come from the two most common kind of unit. The most common situation is that all the neurons in a unit are all ultra-sparse, so that the unit itself responds ultra-sparsely, typically at most one neuron at a time. The second most common situation is where exactly one of the neurons in a unit is in the D population. Then by far the most common response from the unit is due to the single D neuron.

B. Fit with multi-units

To understand how this works, we make a simplified model in which we assume that $R \leq 2$, i.e., that all measured units are either composed of a single neuron or of two neurons. Let p be the fraction of single units. Then, we have for the total probability of a unit responding to k stimuli, ϵ_k^{unit}

$$\epsilon_k^{\text{unit}} = p\epsilon_{k,1}^{\text{unit}} + (1 - p)\epsilon_{k,2}^{\text{unit}}. \quad (33)$$

From the number of single units reported in [32], we estimate $p = 0.34$, and we will use this value from now on.

We then used this in the formalism that we have already set up. The resulting fitted values of the parameters and the χ^2 values are shown in Table IV and, for the case of the hippocampus, the plots of the predicted and recorded n_k are shown in Fig. 6. Compared to the values

	Hipp	EC	Amy	PHC
α_D	$(2.4 \pm 0.3) \times 10^{-2}$	$(3.0 \pm 0.4) \times 10^{-2}$	$(3.4 \pm 0.4) \times 10^{-2}$	$(4.7 \pm 0.5) \times 10^{-2}$
f_D	0.04 ± 0.008	0.03 ± 0.006	0.03 ± 0.006	0.08 ± 0.014
α_{US}	$(6.0 \pm 0.8) \times 10^{-4}$	$(3.2 \pm 0.6) \times 10^{-4}$	$(4.2 \pm 0.7) \times 10^{-4}$	$(3.3 \pm 1.2) \times 10^{-4}$
f_{US}	0.96 ± 0.008	0.97 ± 0.006	0.97 ± 0.006	0.92 ± 0.014
$\chi^2(5)$	1.5	3.0	7.5	14
$\chi^2(10)$	4.9	10.1	15	31

TABLE IV: MLE values and χ^2 values for two-population model, with $0.34N$ single units in each region and $0.66N$ double units in each region.

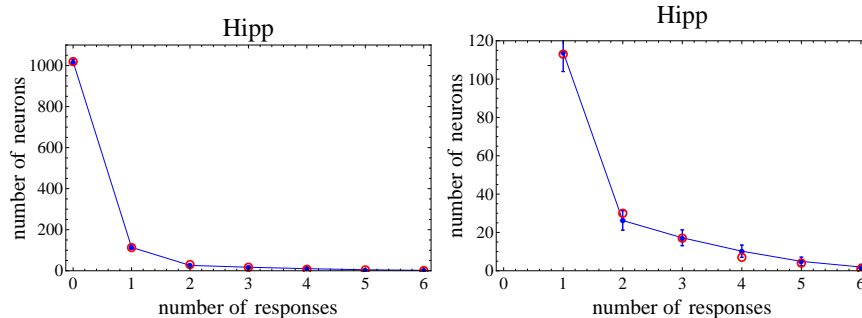


FIG. 6: Plots of MLE fits to the Hipp with the multi-unit model.

fitted for the original two-population model, Table II(c), the χ^2 did not change greatly, although the goodness of fit is somewhat improved, notably in the amygdala and PHC.

Thus the multi-unit model fits all four regions at least as well as the basic two-population model, without any extra fitted parameters. However, the values of some of the parameters did change. Most notably, the estimate of α_{US} decreased by about 40%. The earlier value is simply a weighted average of the effect of single units containing one US neuron with sparsity α_{US} and double units containing two US neurons, with unit sparsity $2\alpha_{US}$. The fitting of the US population is determined primarily from the n_0 and n_1 bins, so the response data by itself cannot significantly determine the existence of these two populations of units; it just gives a weighted average of the sparsities.

In contrast, the value of α_D is only slightly lower than in the earlier fit; this is because most of the relevant data concerns units that have one D neuron. Given the sparseness at the unit level, as in Table II(c), which is tied to measured data, the neural sparsity must be less when there are multiunits.

As to the population fractions, the value f_D is reduced by a factor of about two thirds. This is because for a given f_D at the neural level, there are two chances of having a D neuron in a double unit. Thus the effective value of f_D at the unit level is the following weighted average:

$$f_D(1-p) + 2f_D p = f_D(1+p), \quad (34)$$

which determines the difference between the values of f_D

in Tables II(c) and IV fairly well, given the value $p = 0.34$ that we deduced from Ref. [22].

C. Overall view of effects of multi-units

We see that allowing for multi-units has actually strengthened our conclusion that there is a large fraction of extremely sparsely responding neurons. Effectively the existence of multi-units has diluted the effect in the data relative to the situation at the neural level. The original 2-population fit in Table II(c) characterizes the measured data at the unit level. At the neural level, as supported by Table IV, the fraction of US neurons must be even closer to unity, and their sparsity substantially less than the already small values at the unit level. This qualitative result is independent of the exact numbers of multi-units and the distribution of numbers of neurons in a unit.

VII. DISCUSSION

Our primary result is that in the hippocampus³ (and other areas of the MTL), a vast majority (90% or higher) of neurons respond ultra-sparsely to stimuli in the class presented — around one in a thousand stimuli, or even less. Those neurons that respond more readily, i.e., to

³ In the paper reporting the data we use, it is not stated which hippocampal region the recorded cells belong to.

a few per cent of the stimuli, comprise a rather small fraction (several per cent) of the cells.

We have devised methods that treat the measured neurons and stimuli as statistical samples, and allow the deduction of properties of the ultra-sparse population even though these neurons respond on average to less than a tenth of a stimulus out of the approximately 100 used to obtain the data analyzed [22].

There is the widely-known issue [11, 13, 24, 36, 38] that in many areas of the brain, there appear to be many silent or almost silent cells, i.e., cells that gave no detectable spikes at all in particular experimental situations or that spike very rarely. This gives the problem [24] that responsive neurons reported in the literature can be a very biased sample of all neurons in a probed brain region. Our methods (and potential future improvements) give a way of quantitatively measuring and correcting the bias.

A. Choice of above-threshold responsiveness to define sparsity

Care is needed in interpreting our results. Most importantly, the choice to classify a neuron binarily, as responsive or not, is at its most natural when the neuron normally has a low firing rate and has substantially higher activity under particular circumstances, with fairly few border-line cases.

The simplest case is, of course, when the neuron is strictly binary. That is, it gives exactly zero spikes under normal circumstances, and gives several spikes only in one situation, as for the HVC_{RA} neurons for zebra finches in [11]. But the binary classification is also sensible for cells such as the pyramidal neuron in a human hippocampus whose responses are shown in Fig. 3A of [14]. It gives a consistently high response only to a soaring eagle picture, out of those presented; nevertheless, its response to other presented pictures, while small, is non-zero.

We do not need to commit to the exact semantics of such a neuron to say that the categorical information coded in the high response of the neuron is useful to the subject. This information can be readily used for read-out [7] by a downstream neuron, and therefore used to guide further behavior, etc.

In contrast, for an interneuron such as the one in Fig. 3B of [14], the application of a response threshold is much less sensible. For this neuron the normal state is a fairly high firing rate somewhat correlated with the stimulus and its presentation. One can imagine occasional excursions above some chosen threshold, e.g., the $5\text{-}\sigma$ threshold used in [22]. But if these are only small excursions, their meaning and utility is not obvious. Of course, if under some other specific circumstances not probed in the reported data, the interneuron had a much higher firing rate, then it would be natural to use a thresholded response criterion. This is a situation which our statistical methods are designed to address; if the cell is typical of a

certain class of cells, then one would see examples of the rare large excursions of firing rate in other cell-stimulus combinations.

The above remarks imply that for a better application of our methods, one should extend the criteria for the responsive cells and their responses. Not merely should there be a number of spikes above some threshold relative to the pre-stimulus situation, but the above-threshold distribution of spike numbers should go well above the threshold. It would also be useful to classify cells by their firing rate in the non-responsive state, so that our analysis by populations and sparsity is applied to cells that are similar in characteristics.

B. Populations

We have identified two very different populations of cells in the areas examined. It is possible that these populations are anatomically or functionally different, as with the different kinds of cells in the HVC and RA areas of zebra finches [11, 16]. But this is not a necessary deduction. Indeed, we think that is unlikely that our two populations correspond directly to the pyramidal cell and interneuron populations reported in [14]. The presence of the different populations might simply represent different semantic properties for the cells' firing relative to the nature of the particular class of stimuli used. One can at best assume only that the situation is typical. For example, suppose one chose stimuli in a different class, e.g., musical tunes instead of famous people. Then some cells that had very low sparsity in the famous-people situation could have much higher sparsity in the music situation, and vice versa. Since such changing contexts are common experience, it is reasonable that this situation is typical. The different populations correspond to different semantic domains, and the chosen stimuli sample these domains.

The populations and their sparsities must then be treated as being relative to the general class of stimuli used, e.g., famous individuals, landmarks, animals or objects in the case of the data from [22] that we analyzed.

C. Cell semantics

It has been suggested that the neurons under discussion are concept cells [29]; each cell responds to the presence, in some sense, of a particular concept in the current stimulus. One part of the motivation for this is that the responses often appear to be genuinely conceptual; for example, a cell might respond (within the experimental data) only to stimuli involving a particular person, e.g., to multiple different pictures of the person, even in disguise, to the written name of the person, and to the spoken name.

In this section, we make some suggestions about how our results quantitatively impact this issue. We label the

subject that of the semantics of the cells, i.e., of what meaning should be attached to their responses.

In the first place our results strengthen the basic case for conceptual cells, by showing how sparse the responses typically are. However, this case can only be made in conjunction with the measurements of the conceptual properties of the responses. To understand this more clearly, it is important to recall that there are two kinds of measurement involved.

First, there are screening sessions, with many different unrelated stimuli. The number of different objects and people averaged to 97, and it was our analysis of this data that led to our deduction that there are many very sparsely firing cells.

The screening sessions find pairs of stimulus and neuron where a high response is obtained. Then, in testing sessions, variants on the response-causing stimuli were used. It is the testing sessions that establish that many responses are indeed conceptual — e.g., a neuron responds to a picture, the written name, and to the spoken name of a particular human. However, it is the screening session data that determine the sparseness of the cells' responses, because the screening sessions have the largest number of identifiably distinct concepts.

It is tempting to say that because a cell consistently responds to a variety of very different stimuli related to a particular person, e.g., Jennifer Aniston [32], that the cell actually represents Jennifer Aniston, i.e., that its firing above threshold codes that the concept of Jennifer Aniston is being processed or has been detected. This is the simplest version of the concept cell idea [29].

We now address three questions about the exact correctness of this interpretation: One is whether the concept involved is in fact the obvious one, e.g., Jennifer Aniston in the case just mentioned. The second is whether the concept is one that in some sense corresponds to the current stimulus, be it visual or auditory. Our third question is whether the neural conceptual representation is strictly local, i.e., whether the above-threshold firing of one of these cells codes only a single concept. Our discussion of these questions will provoke a fourth question: Whether the representation for only one concept is active at a given time is active or whether the representations of multiple concepts are (more-or-less) simultaneously active, on a time scale of a few hundred milliseconds.

First it appears necessary that a concept, like Jennifer Aniston, is coded and represented in the subject's brain. But the reported cell can be a downstream consequence. For example, it might code the activation of an episodic memory of a show in which she participated. Evidently, such downstream activated concepts are related to the Jennifer Aniston concept. Support of the idea that the apparent concept cells may code downstream concepts is that the Jennifer Aniston cell was later found [29] to respond to a picture of Lisa Kudrow, a co-star of Aniston's in a television series. That individual episodic memories may be among the concepts involved (for some appro-

priate definition of "concept") is suggested because of the well-known central role of the hippocampus in the episodic memory system.

We know that, at least in humans, recall of memories can be based not directly on a current stimulus but on cues generated by internal cognition. In general, this removes an obligatory link between stimulus properties and conceptual neural responses. For the experimental measurements under discussion, this issue need not be important, because the experimental protocol was explicitly designed to have the subjects' attention focused on the stimuli.

Once one allows that downstream concepts are activated, one should expect that multiple concepts are simultaneously active, with perhaps only one being selected at a given time for conscious attention. This is essentially the same property that computer search engines have. We can regard these as associative memory systems. A cue, e.g., a search string, is provided as input, and the result is a list of items containing or related to the cue; these are the activated concepts. The user can click on one item in the list to get its content; this is analogous to conscious memory recall.

The next question is whether or not the representation is local. Normally a dichotomy is made simply between local representations and distributed representations. In the case of distributed representations, even when they are sparse, it is generally assumed that the individual neurons that are involved in a distributed representation of an object themselves represent features or properties of the object in question — see, for example, Ref. [10, 23] and references therein. Such representations were called "iconic" by Wickelgren [41–43].

But a further possibility is the use of what Wickelgren [41–43] called "chunk assemblies". Each of these is a relatively small set of cells, the activation of which codes the presence or processing of the associated concept. The individual cells in a chunk assembly do not themselves code features corresponding to the concept. This provides an important modification to the concept-cell idea. Quantitatively, coding using chunk assemblies is characterized by the number of cells in each assembly and by the number of chunk assemblies in which each cell participates (which need not be exactly fixed numbers). Local coding is the limiting case in which each cell participates in the assembly for exactly one concept, as opposed to participating in merely a very small fraction of the concepts stored in a system. We can regard our work as a step in determining quantitative properties of chunk assemblies. When only a small number of stimuli are used, a cell in a chunk assembly will behave quite similarly to a cell providing a local representation.

We now work out a relation between the sparsity of cell responses, and some of the coding properties. The properties of interest are the total number of concepts coded, the number of concepts that each cell codes (i.e., the number of chunk assemblies it participates in), and the number of concepts that are simultaneously active.

Of course neither of the last two numbers need be fixed, but it will be useful to treat them as single or representative numbers to get an idea of the relation to sparsity. If only one concept were active at a time, and if the coding were local (so there is only one concept per cell), then the sparsity would be $1/\text{Total \# concepts}$.

With the possibilities of multiple concepts being simultaneously active and of more the one concept being coded per cell, we get instead:

$$\text{sparsity} = \frac{(\# \text{ concepts activated}) (\# \text{ concepts per cell})}{\text{Total \# concepts}}, \quad (35)$$

at least in some average sense, given that both the number of concepts activated and the number stored by the cell are small compared with total number of concepts stored overall. The number of concepts per cell in the case of a local representation is unity. The simplest ideas about local/grandmother-cell representations would also assign unity to the number of simultaneously active concepts. Given the number of concepts we should expect to be represented in the human brain (probably hundreds of thousands if not millions), even our small measured sparsity is much too large to be consistent with a local representation. In this discussion, we should use the word ‘‘concept’’ very broadly, such that it includes, for example, individual episodic memories.

Now an estimate of 10,000 to 30,000 has been quoted by Waydo et al. [40] as the number of objects that a typical adult recognizes, on the basis of work by Biederman [3]. But this is surely a substantial underestimate of the number of concepts that are coded in a human brain. First, the number of words in a language that known to an adult is in the tens of thousands, and the number of concepts is surely substantially higher. Second, it is known that humans can remember thousands of pictures [15, 37] presented during a single day. The total number of memories created over a lifetime must be orders of magnitude larger. Even allowing that on a long time scale many of these will be forgotten, this indicates that the number of concepts/objects represented can easily be in the hundreds of thousands or millions.

For illustration assume that the number of concepts remembered is 10^6 . Then a measured sparsity of around 6×10^{-4} , as we found for the majority population from our analysis, implies that

$$(\# \text{ concepts activated}) \times (\# \text{ concepts per cell}) \simeq 600. \quad (36)$$

We leave further analysis to the future, but use this estimate as a suggestion about the quantitative properties of concept coding.

D. Confirmation and relation to previous work

Our results confirm and substantially strengthen results found by one of us and Jin in [9]. There we used earlier data from [32] that only provided values for the

number of units with one response, N_1 , the number with two or more responses, $N_{\geq 2}$, and for the average number of responses from responsive units. We ruled out a one-population model, and fit the three parameters of the two-population model from the three reported summary statistics. But there was therefore no test of goodness of fit for the 3-parameter model. Instead the shape of the N_k distribution was a prediction, which is successfully tested in this paper, for the case the hippocampus and entorhinal cortex, at least.

In the present paper, we also give a more systematic account of the statistical methods, and have a breakdown by brain region, using newer data. Although the exact parameters of the fits are a little different, the main picture is confirmed and tested. The differences could be accounted for by differences in the subjects and of detailed experimental procedures and by our different treatment of multiunits.

E. Treves-Rolls definition of sparseness

An alternative measure of sparseness proposed by Rolls and Tovee [34] and reviewed by Treves and Rolls [35], is calculated from the firing rates of neurons in response to stimuli. The average sparseness reported [35] with this definition was 0.34 ± 0.13 (for hippocampal spatial view cells in the macaque hippocampus). This is dramatically different than what we found with our definition of sparsity. It is worth understanding how this difference might arise (aside from a conceivable difference between species). We will demonstrate that the Treves-Rolls definition can be very misleading as to the nature of neural coding.

They define the sparseness of a neuron in response to a sample of S stimuli as

$$a_{\text{TR}}^s = \frac{\langle r \rangle^2}{\langle r^2 \rangle} = \frac{\left(\sum_{j=1} r_j / S \right)^2}{\left(\sum_{j=1} r_j^2 \right) / S}, \quad (37)$$

where r_j is the mean firing rate of the neuron in response to stimulus j and $\langle \dots \rangle$ denotes an average of a quantity over all presented stimuli. In the case that the neuron is binary in its responses, i.e., that it gives a large response with some fixed firing rate to some stimuli and is exactly silent for all other stimuli, this definition gives the same result as our definition of sparsity.

Note, however, that there is a difference that the above definition is applied to one neuron with the stimuli actually presented in an experiment, whereas ours applies for a universe of stimuli. Our sparsity is something that must be inferred from statistical arguments applied to data, whereas theirs is directly defined as a property of the data. Even so, if neurons are *exactly* binary and all have the same sparsity (in our sense), then the Treves-Rolls sparsity is a good estimator of our sparsity.

The definition (37) is in fact the unique combination of the first and second moments of the firing rate that

gives α for exactly binary neurons (always in the limit of large S). However, as we will now show, Rolls-Treves sparseness and our thresholded sparsity can have widely different values if the neurons are not strictly binary.

We first observe that Rolls and Treves only reported a value of sparsity averaged over all neurons. Now Ison et al. [14] in their Fig. S2 showed the distribution across neurons of various measures of sparseness and selectivity. There is a wide range of Rolls-Treves sparseness from less than 0.1 (the most common) to another peak close to 1 (for putative interneurons). The average of this distribution is quite misleading as to the properties of individual neurons. Furthermore, all the distributions in that figure are measures of sparseness with respect to the presented stimuli, and no attempt is made to infer an underlying sparseness or selectivity defined with respect to a whole class of stimuli, such as we do here and Waydo et al did in [40].

It is well known that many (but not all) hippocampal neurons respond strongly to certain specific behaviorally relevant stimuli or situations, while responding weakly or not at all at other times. The data we analyzed simply give a particularly notable example. Let us refer to the situations to which a cell responds strongly as “on-target” and the other situations as “off-target”. Suppose, that the on-target responses are very rare, as we have found, but that the off-target responses, while being of low rate, are nevertheless non-zero. For example, the hippocampal place cells found in rats are known to have dramatically different firing rates when an animal is in the place field of the cell (producing an on-target response) compared to when the subject is out of the place field (producing an off-target response).

We will now point out by constructing an appropriate class of models that the Treves-Rolls sparseness can be dominated by properties of the off-target firing while being quite insensitive to the on-target responses. At the same time, an appropriate choice of threshold can make it quite unambiguous as to which responses are on-target and which are off-target. The model is intended not to be (at this point) an actual representation of data, but just a reasonable counterexample, to show how a high average value of Rolls-Treves sparseness can be compatible with a very low sparsity in our sense.

In this model each neuron has a categorical response to a certain class of stimuli, with probability α . But instead of assuming purely binary neurons, we postulate a pseudo-binary model in which the on-target and off-target firing both come from a distribution of firing rates, but with different distributions. Let us assume that the off-target and on-target firing rates have the distributions $P_0(r)$ and $P_1(r)$ respectively.⁴ Then the total distribu-

tion is a mixture:

$$P(r) = (1 - \alpha)P_0(r) + \alpha P_1(r). \quad (38)$$

We let r_0 and Δr_0 be the mean and standard deviation of the off-target responses, and let r_1 and Δr_1 be the same quantities for the on-target responses. Naturally, we should assume that r_1 is sufficiently much higher than r_0 that on-target responses can be detected adequately reliably; this depends on the tail of $P_0(r)$ falling sufficiently rapidly as r increases.

A calculation yields the Rolls-Treves sparseness (relative to all stimuli) as:

$$\begin{aligned} a_{\text{TR}}^s &= \frac{\left(1 + \frac{\alpha}{1 - \alpha} \frac{r_1}{r_0}\right)^2}{\frac{1}{1 - \alpha} \left(1 + \frac{(\Delta r_0)^2}{r_0^2}\right) + \frac{\alpha}{(1 - \alpha)^2} \left(\frac{r_1^2}{r_0^2} + \frac{(\Delta r_1)^2}{r_0^2}\right)}. \end{aligned} \quad (39)$$

This reproduces the value α in the case of binary neurons, i.e., where the standard deviations are negligible and the limit $r_0 \rightarrow 0$ is taken. But if instead we take the situation that α is very small (much less than the ratio r_0/r_1 of off- to on-target mean responses), then the Treves-Rolls sparseness approaches $1/(1 + \Delta r_0^2/r_0^2)$. This is just the Rolls-Treves sparseness calculated purely from the off-target distribution. In this case the Rolls-Treves sparseness says nothing about the on-target responses.

If the two distributions P_0 and P_1 are distinct enough, then it is possible to set a threshold r_{th} to give reliable detection of on-target and off-target states. Given an off-target stimulus, we need the false positive rate to be substantially less than α , so that above threshold responses are predominantly for on-target stimuli. This requires

$$\int_{r_{\text{th}}}^{\infty} P_0(r) dr \ll \alpha, \quad (40)$$

i.e., that the threshold is sufficiently far out on the tail of P_0 .

Given an on-target stimulus, we need it to be reliably detected, so that the false negative rate (relative to α) is small, i.e.,

$$\int_0^{r_{\text{th}}} P_1(r) dr \ll 1. \quad (41)$$

This is arranged if the bulk of the on-target distribution is beyond the threshold.

For any given value of α we can arrange to satisfy all these conditions with appropriate functions for the

⁴ Analysis of a large, unbiased set of neurons in the rat MTL reported in [21] suggests a log-normal distribution for both $P_0(r)$ and $P_1(r)$. However, the exact forms of the distributions $P_0(r)$

and $P_1(r)$ are not important in this analysis, so long as they are largely non-overlapping.

two underlying distributions $P_0(r)$ and $P_1(r)$. That is, the Rolls-Treves sparseness can be dominated by its off-target value, while we have reliable discrimination between on-target and off-target stimuli, despite the low proportion α of on-target stimuli.

In this situation, there is no contradiction between a rather high value of Rolls-Treves sparseness, like 0.3 and extremely low values of our sparsity. Given the behavioral significance of the above-threshold responses in [32], it is sparsity in our sense that is most relevant to understanding the nature of the corresponding conceptual coding.

F. What properties of neural responses are determined?

Although our model provides a good fit to the data (at least in the hippocampus and entorhinal cortex), it should not be supposed that the model gives an exact characterization of neural responses to stimuli.

The first issue is simply that if we replaced one particular neural population of a particular sparsity α and fractional abundance f by several populations with sparsities not too far from the original single value, and with a total abundance summing to f , the result would not be very distinguishable from the original case. In the limit of a large number of stimuli, the number of responses from one population would be clustered at $k = \alpha S$, with a standard deviation $\sqrt{\alpha S}$ that is much smaller than the mean. The *fractional* standard deviation is $1/\sqrt{\alpha S}$. But with the actual values of S and α , the standard deviation is comparable to the mean; indeed, for the ultra-sparse population the standard deviation is much larger than the mean. Thus splitting one population into a set of populations nearby in sparsity produces little measurable effect.

The lack of ability to distinguish populations of nearby sparsity is particularly notable for the ultra-sparse population. This populates primarily the $k = 1$ bin. Thus our measurement of a sparsity for the ultra-sparse population is really a measurement of a weighted average of the sparsities of the ultra-sparsely responding neurons.

What is properly deduced from our analysis is that there are relatively few neurons that respond with a sparsity of a few per cent, and a much larger number that respond much more sparsely.

A more precise understanding of how the multiunit cases arise from an underlying neural response — e.g., [8] — would lead to a more precise estimation of the population parameters at the neural level.

A second issue [11, 13, 24, 36, 38] is that there may be many silent cells, i.e., cells that gave no detectable spikes at all in the measurements. Silent cells are to be contrasted with the many non-responsive cells that were included and were important in our analysis; non-responsive cells did give detected spikes, but never enough to count as an above-threshold response. On the

basis of results in [13], Waydo et al. [40] argue that this is potentially a very large effect. They suggest that “as many as 120–140 neurons are within the sampling region of a tetrode in the CA1 region of the hippocampus”, but say that they only identified “1–5 units per electrode”. Of course some of these units are multiunits, corresponding to two or more neurons.

To quantify the effects of silent cells, let K be the ratio the total number of cells to the number of detected cells. The suggestion [13, 36, 40] is that K could be as much as an order of magnitude. The effect of silent cells on our measurement of the sparsity α_D of the higher sparsity population would be negligible. This is simply because these cells typically respond to multiple stimuli in the data, and are actually detected. The value of α_D is obtained primarily from the relative numbers of cells with $k = 2$, $k = 3$, etc responses. But their fraction in the total neuronal population, f_D must be decreased by a factor K .

For the ultra-sparse population, the sparsity α_{US} is decreased relative to our fits by a factor K (while the population abundance gets closer to 100%). This is simply because α_{US} is, to a first approximation, the ratio of N_1 to $N_0 + N_1$ (after taking out the estimated contamination of these bins from the other population). N_1 is fixed by data, but $N_0 + N_1$ is increased by a factor of about K . Effectively, if there is a population of completely silent cells, then the measured number N_0 of cells that gave no above-threshold responses should be changed to approximately KN_0 . (The approximations consist of neglecting N_1 with respect to N_0 and neglecting the small number of cells in the D population for which all the stimuli were off-target.)

The effect of possible large numbers of silent cells is to substantially strengthen our conclusions, even if it makes some of the numbers less certain. Of course, if at some time in the future, a more precise understanding of electrode properties were obtained, then a useful estimate of the silent cell factor K could be obtained. After that our numerical results could be adjusted accordingly. See [8, 25] for recent work on this issue.

A final issue is that the measurements of sparsity are relative to a particular set of stimuli. We need to regard the stimuli as being chosen as a sample from an enormous number in a general subject area known to the patient. The general topics were chosen to correspond to areas that were well known to the subjects. Given that the neural responses were very specific, one must suppose that if a very different topic were chosen (e.g., scientific subjects instead of movie stars), the responses (or lack thereof) by particular neurons could be very different. Some previously responsive cells might even become silent, and vice versa. Similar phenomena are seen with place field behavior of hippocampal neurons when an animals environment is changed [17]. So any estimate of the sparsity of the response of a particular neuron is relative to the subject area of the stimuli. Nevertheless, it is reasonable that the distribution of sparsity across a

population of hippocampal neurons would be not much changed between different stimuli sets.

It is known that the hippocampus is involved generally in episodic memory, so over the whole neural population one should expect to get responses to stimuli of all subject areas. There should not be specialization for the particular subject areas used for the measurements except for the fact that the topics are ones for which the

subjects have abundant memories. Therefore our results concerning the neuronal population as a whole should be regarded as broadly applicable. That is, we should expect similar results for other topics for the stimuli. This conclusion also makes it acceptable that we analyzed data not just from one patient but data pooled over many patients.

Appendix A: Poisson approximation for likelihood

We now review the derivation of the Poisson approximation (15) to the likelihood function (12). The derivation applies when the values of ϵ_k for non-zero k are small, more precisely, when $\sum_{k=1}^S \epsilon_k \ll 1$.

We start from Eq. (12) by factoring out the $k = 0$ factors from the product, and then using Eqs. (13) and (14) to write n_0 and ϵ_0 in terms of the corresponding quantities for $k \geq 1$:

$$\mathcal{L}(\{\alpha_i, f_i\}) = \frac{N!}{(N - n_{\geq 1})!} (1 - \epsilon_{\geq 1})^{N - n_{\geq 1}} \prod_{k=1}^S \frac{\epsilon_k^{n_k}}{n_k!}, \quad (\text{A1})$$

where $n_{\geq 1} = \sum_{k=1}^S n_k$, and $\epsilon_{\geq 1} = \sum_{k=1}^S \epsilon_k$. By taking the logarithm of both sides of Eq. (A1) we get:

$$\ln \mathcal{L} = \ln N! - \ln[(N - n_{\geq 1})!] + (N - n_{\geq 1}) \ln(1 - \epsilon_{\geq 1}) + \ln \prod_{k=1}^S \frac{\epsilon_k^{n_k}}{n_k!}. \quad (\text{A2})$$

For large N , we can use Stirling's approximation to $O(1/N)$:

$$\ln N! = N \ln N - N + \frac{1}{2} \ln(2\pi N) + O\left(\frac{1}{N}\right). \quad (\text{A3})$$

Applying this formula to the first two terms in (A2) yields

$$\begin{aligned} \ln \mathcal{L} &= N \ln N + (N - n_{\geq 1}) \ln\left(\frac{1 - \epsilon_{\geq 1}}{N - n_{\geq 1}}\right) - n_{\geq 1} + \ln \prod_{k=1}^S \frac{\epsilon_k^{n_k}}{n_k!} + O\left(\frac{1}{N}\right) \\ &= n_{\geq 1} \ln N + (N - n_{\geq 1}) \ln\left(1 - \frac{\epsilon_{\geq 1} - n_{\geq 1}/N}{1 - n_{\geq 1}/N}\right) - n_{\geq 1} + \ln \prod_{k=1}^S \frac{\epsilon_k^{n_k}}{n_k!} + O\left(\frac{1}{N}\right). \end{aligned} \quad (\text{A4})$$

(The approximation worsens beyond the order $1/N$ error estimate if $n_{\geq 1}$ gets close to N . But since the ϵ_k are small, this situation is of very low probability. Henceforth the error estimates will apply not too far from the peak of the likelihood distribution.)

The first term can be combined with the product term

$$n_{\geq 1} \ln N + \ln \prod_{k=1}^S \frac{\epsilon_k^{n_k}}{n_k!} = \ln \left[N^{n_{\geq 1}} \prod_{k=1}^S \frac{\epsilon_k^{n_k}}{n_k!} \right] = \ln \prod_{k=1}^S \frac{(N \epsilon_k)^{n_k}}{n_k!}. \quad (\text{A5})$$

We can simplify the remaining logarithm in Eq. (A4)

$$(N - n_{\geq 1}) \ln\left(1 - \frac{\epsilon_{\geq 1} - n_{\geq 1}/N}{1 - n_{\geq 1}/N}\right) = (N - n_{\geq 1}) \left(\frac{n_{\geq 1}/N - \epsilon_{\geq 1}}{1 - n_{\geq 1}/N} + O\left[\left(\frac{\epsilon_{\geq 1} - n_{\geq 1}/N}{1 - n_{\geq 1}/N}\right)^2\right] \right). \quad (\text{A6})$$

For a multinomial distribution,

$$\epsilon_{\geq 1} - n_{\geq 1}/N = \sum_{k=1}^S (\epsilon_k - n_k/N) = \sum_{k=1}^S O\left(\sqrt{\epsilon_k/N}\right), \quad (\text{A7})$$

where we have used the standard deviation of the distribution to estimate the typical value of $|\epsilon_k - n_k/N|$.

Thus we can write:

$$O \left[\left(\frac{\epsilon_{\geq 1} - n_{\geq 1}/N}{1 - n_{\geq 1}/N} \right)^2 \right] = O \left[\frac{1}{N} \left(\sum_{k=1}^S \sqrt{\epsilon_k} \right)^2 \right] = O(\epsilon_{\geq 1}/N). \quad (\text{A8})$$

Thus, Eq. (A6) can be simplified to:

$$(N - n_{\geq 1}) \ln \left(1 - \frac{\epsilon_{\geq 1} - n_{\geq 1}/N}{1 - n_{\geq 1}/N} \right) = n_{\geq 1} - N\epsilon_{\geq 1} + O(\epsilon_{\geq 1}) + O(1/N) \quad (\text{A9})$$

Substituting Eqs. (A5) and (A9) into Eq. (A4) yields

$$\ln \mathcal{L} = -N\epsilon_{\geq 1} + \ln \prod_{k=1}^S \frac{(N\epsilon_k)^{n_k}}{n_k!} + O(\epsilon_{\geq 1}) + O(1/N). \quad (\text{A10})$$

Therefore the likelihood function in our approximation is given by a product of Poisson distributions:

$$\mathcal{L} \approx \prod_{k=1}^S e^{-N\epsilon_k} \frac{(N\epsilon_k)^{n_k}}{n_k!}. \quad (\text{A11})$$

-
- [1] D. Attwell and S.B. Laughlin, “An Energy Budget for Signaling in the Grey Matter of the Brain”, *J. Cereb. Blood Flow Metab.* **21**, 1133–1145 (2001).
- [2] S. Baker and R.D. Cousins, “Clarification of the Use of Chi-Square and Likelihood Functions in Fits to Histograms”, *Nucl. Instrum. Meth.* **221**, 437–442 (1984).
- [3] I. Biederman, “Recognition-by-Components: A Theory of Human Image Understanding”, *Psychol. Rev.* **94**, 115–147 (1987).
- [4] J. Bowers, “On the Biological Plausibility of Grandmother Cells: Implications for Neural Network Theories in Psychology and Neuroscience”, *Psychol. Rev.* **116**, 220–251 (2009).
- [5] J. Bowers, “More on Grandmother Cells and the Biological Implausibility of PDP Models of Cognition: A Reply to Plaut and McClelland (2010) and Quian Quiroga and Kreiman (2010)”, *Psychol. Rev.* **117**, 300–306 (2010).
- [6] J. Bowers, “Postscript: Some Final Thoughts on Grandmother Cells, Distributed Representations, and PDP Models of Cognition”, *Psychol. Rev.* **117**, 306–308 (2010).
- [7] G. Buzsáki, “Neural Syntax: Cell Assemblies, Synapses, and Readers”, *Neuron* **68**, 362–385 (2010).
- [8] L.A. Camuñas-Mesa and R.Q. Quiroga, “A Detailed and Fast Model of Extracellular Recordings”, *Neural Comput.* **25**, 1191–1212 (2013).
- [9] J. Collins and D.Z. Jin, “Grandmother cells and the storage capacity of the human brain”, arXiv:q-bio/060301.
- [10] P. Földiák and D. Endres, “Sparse coding”, *Scholarpedia*, 3(1):2984 (2008).
- [11] R.H.R. Hahnloser, A.A. Kozhevnikov, and M.S. Fee, “An ultra-sparse code underlies the generation of neural sequences in a songbird”, *Nature* **419**, 65–70 (2002).
- [12] T. Hauschild and M. Jentzel, “Comparison of maximum likelihood estimation and chi-square statistics applied to counting experiments”, *Nucl. Instrum. Meth.* **457**, 384–401 (2001).
- [13] D.A. Henze, Z. Borhegyi, J. Csicsvari, A. Mamiya, K.D. Harris, and G. Buzsáki, “Intracellular Features Predicted by Extracellular Recordings in the Hippocampus In Vivo”, *J. Neurophysiol.* **84**, 390–400 (2000).
- [14] M.J. Ison, F. Mormann, M. Cerf, C. Koch, I. Fried, and R.Q. Quiroga, “Selectivity of pyramidal cells and interneurons in the human medial temporal lobe”, *J. Neurophysiol.* **106**, 1713–1721 (2011).
- [15] T. Konkle, T.F. Brady, G.A. Alvarez, and A. Oliva, “Conceptual Distinctiveness Supports Detailed Visual Long-Term Memory for Real-World Objects” *J. Exp. Psychol. Gen.* **139**, 558–578 (2010).
- [16] A.A. Kozhevnikov and M.S. Fee, “Singing-Related Activity of Identified HVC Neurons in the Zebra Finch”, *J. Neurophysiol.* **97**, 4271–4283 (2007).
- [17] I. Lee, G. Rao, and J.J. Knierim, “A Double Dissociation between Hippocampal Subfields: Differential Time Course of CA3 and CA1 Place Cells for Processing Changed Environments”, *Neuron*, Vol. 42, 803–815, (2004).
- [18] P. Lennie, “The Cost of Cortical Computation”, *Curr. Biol.* **13**, 493–497 (2003).
- [19] L. Lyons, “Statistics for Nuclear and Particle Physicists” (Cambridge University Press, 1986).
- [20] J.F. Miller, M. Neufang, A. Solway, A. Brandt, M. Trippel, I. Mader, S. Hefft, M. Merkow, S.M. Polyn, J. Jacobs, M.J. Kahana, A. Schulze-Bonhage, “Neural Activity in Human Hippocampal Formation Reveals the Spatial Context of Retrieved Memories”, *Science* **342**, 1111–1114 (2013).
- [21] K. Mizuseki and G. Buzsáki, “Preconfigured, Skewed

- Distribution of Firing Rates in the Hippocampus and Entorhinal Cortex”, *Cell Rep.* **4**, 1–12 (2013).
- [22] F. Mormann, S. Kornblith, R.Q. Quiroga, A. Kraskov, M. Cerf, I. Fried, and C. Koch, “Latency and Selectivity of Single Neurons Indicate Hierarchical Processing in the Human Medial Temporal Lobe”, *J. Neurosci.* **28**, 8865–8872 (2008).
- [23] B.A. Olshausen and D.J. Field, “Sparse Coding of Sensory Inputs”, *Curr. Opinion Neurobiol.* **14**, 481–487 (2004).
- [24] B.A. Olshausen and D.J. Field, “How Close Are We to Understanding V1?”, *Neural Comput.* **17**, 1665–1699 (2005); “What is the other 85% of V1 doing?”, in “23 problems in systems neuroscience”, J.L. van Hemmen and T.J. Sejnowski (eds.) (Oxford University Press, 2006).
- [25] C. Pedreira, J. Martinez, M.J. Ison and R. Quian Quiroga, “How many neurons can we see with current spike sorting algorithms?”, *J. Neurosci. Meth.* **211**, 58–65 (2012).
- [26] D.C. Plaut and J.L. McClelland, “Locating Object Knowledge in the Brain: Comment on Bower’s (2009) Attempt to Revive the Grandmother Cell Hypothesis”, *Psychol. Rev.* **117**, 284–288 (2010).
- [27] D.C. Plaut and J.L. McClelland, “Postscript: Parallel Distributed Processing in Localist Models Without Thresholds”, *Psychol. Rev.* **117**, 289–290 (2010).
- [28] R.Q. Quiroga, “Decoding Visual Inputs From Multiple Neurons in the Human Temporal Lobe”, *J. Neurophysiol.* **98**, 1997–2007 (2007).
- [29] R.Q. Quiroga, “Concept cells: the building blocks of declarative memory functions”, *Nat. Rev. Neurosci.* **13**, 587–597 (2012).
- [30] R.Q. Quiroga and G. Kreiman, “Measuring Sparseness in the Brain: Comment on Bowers (2009)”, *Psychol. Rev.* **117**, 291–297 (2010).
- [31] R.Q. Quiroga and G. Kreiman, “Postscript: About Grandmother Cells and Jennifer Aniston Neurons” *Psychol. Rev.* **117**, 297–299 (2010).
- [32] R.Q. Quiroga, L. Reddy, G. Kreiman, C. Koch, and I. Fried, “Invariant visual representation by single neurons in the human brain”, *Nature* **435**, 1102–1107 (2005).
- [33] E.T. Rolls, “The mechanisms for pattern completion and pattern separation in the hippocampus,” *Front. Syst. Neurosci.* **7**, 74 (2013).
- [34] E.T. Rolls and M. Tovee, “Sparseness of the Neuronal Representation of Stimuli in the Primate Visual Cortex”, *J. Neurophys.* **73**, 713–726 (1995).
- [35] E.T. Rolls and A. Treves, “The neuronal coding of information in the brain”, *Prog. Neurobiol.* **95**, 448–490 (2011).
- [36] S. Shoham, D.H. O’Connor, and R. Segev, “How silent is the brain: is there a “dark matter” problem in neuroscience?”, *J. Comp. Physiol. A* **192**, 777–784 (2006)
- [37] L. Standing, “Learning 10,000 pictures”, *Q. J. Exp. Psychol.* **25**, 207–222 (1973).
- [38] L.T. Thompson and P.J. Best, “Place Cells and Silent Cells in the Hippocampus of Freely-Behaving Rats”, *J. Neurosci.* **9**, 2382–2390 (1989).
- [39] A. Treves and E.T. Rolls, “What determines the capacity of autoassociative memories in the brain?”, *Network* **2**, 371–397 (1991).
- [40] S. Waydo, A. Kraskov, R. Quian Quiroga, I. Fried, and C. Koch, “Sparse Representation in the Human Medial Temporal Lobe”, *J. Neurosci.* **26**, 10232–10234 (2006).
- [41] W.A. Wickelgren, “Learned specification of concept neurons”, *Bull. Math. Biophys.* **31**, 123–142 (1969).
- [42] W.A. Wickelgren, “Webs, Cell Assemblies, and Chunking in Neural Nets”, *Concepts in Neuroscience* **3**, 1–53 (1992).
- [43] W.A. Wickelgren, “Webs, Cell Assemblies, and Chunking in Neural Nets: Introduction”, *Can. J. Exper. Psych.* **53** 118–131 (1999).